Polymer Maximum Drag Reduction: A Unique Transitional State

Yves Dubief[1], C. M. White[2], E. S. G. Shaqfeh[3] and V. E. Terrapon[4]

[1]*School of Engineering, University of Vermont, Burlington VT*
[2]*Department of Mechanical Engineering, University of New Hampshire, Durham NH*
[3]*Department of Mechanical Engineering, Stanford University, Stanford CA*
[4]*Aerospace and Mechanical Engineering Department, University of Liege, Belgium*
(Dated: June 23, 2011)

The upper bound of polymer drag reduction is identified as a unique transitional state between laminar and turbulent flow corresponding to the onset of the nonlinear breakdown of flow instabilities.

PACS numbers: Valid PACS appear here

Drag reduction by the addition of long-chain polymers to flowing liquids is bounded by the so-called maximum drag reduction (MDR) asymptote [1]. Drag reductions attained at MDR may be as high as 80% in turbulent boundary layers and channel flows over smooth plane walls, and as such, MDR has received extensive research interest. One characteristic of MDR is that the mean velocity profile, determined empirically by Virk *et al.*[1] as:

$$\overline{u}^+ = 11.7\log(y^+) - 17, \qquad (1)$$

is found to be roughly universal, insensitive to polymer species, molecular weight, or the polymer-solvent pair. The superscript $^+$ in Eq. (1) denotes normalization by the friction velocity $u_\tau = \sqrt{\tau_w/\rho}$ and kinematic viscosity ν, where τ_w is the shear stress at the wall and ρ the fluid density. While the universality of the Virk profile is generally well-accepted, a point of controversy is the behavior of the Reynolds shear stress at MDR. Warholic *et al.*[2] measured virtually no Reynolds shear stress and conjectured that MDR corresponds to the state where Reynolds stresses are negligible and turbulence is sustained by polymer stresses. However, Ptasinski *et al.* [3] reports a reduced, yet finite Reynolds shear stress at MDR, corresponding to approximately a 50% reduction in maximum Reynolds shear stress compared to a Newtonian flow. Nevertheless, despite the differences in high-order turbulence statistics, both experiments find a mean velocity profile that agrees reasonably well with Eq. (1). The question therefore arises whether MDR is uniquely defined and, as such, can it be uniquely predicted. The answer to this question is important not only to better understand the bounding mechanisms of MDR but also to develop robust models to predict drag reduction given an initial set of conditions.

This letter tests and demonstrates the hypothesis that MDR is a unique transitional state between laminar and turbulent flow and that the state of turbulence at MDR can be extrapolated by the mechanisms of polymer-vortex interactions framed by Dubief et al.[4], Terrapon *et al.*[5] and Kim et al.[6]. A necessary condition of our hypothesis is the existence of transitional states in a Newtonian fluid with velocity statistics similar to MDR states observed experimentally [2, 3]. To demonstrate that this condition is satisfied, we have analyzed the DNS data of bypass transition in a boundary layer flow of Wu & Moin[7]. Fig. 1a indicates that the region between $Re_\theta = 200$ and 300 best approaches Virk's asymptotic velocity profile. Here the Reynolds number, Re_θ, is based on the momentum boundary layer thickness θ. Shown in Fig. 1b is that from $Re_\theta = 200$ to $Re_\theta = 300$, the Reynolds shear stress increases from almost negligible levels ($\lesssim 10\%$) of the full turbulent state to roughly half the fully turbulent level. In between these two states, the skin friction C_f (Fig. 1c) reaches a minimum, which marks the end of the instability stage and the beginning of the nonlinear development stage. Collectively, these data suggest that the MDR state may correspond to a narrow region near the beginning of the nonlinear breakdown stage, including pre- and post-breakdown stages. They are also suggestive that the variations in high-order turbulence statistics, such as Reynolds shear stress, observed experimentally at MDR may likely be a consequence of the transitioning between pre- and post-breakdown stages when computing averaged turbulence statistics.

Viewed from the framework of the underlying fluid structure, the nonlinear breakdown stage is associated with the breakdown of the near-wall low- and high-speed velocity streaks and the subsequent generation of near-wall quasi-streamwise vortices. Once triggered, the wall-shear, velocity streaks, and quasi-streamwise vortices form the autonomous self-sustaining cycle of wall turbulence [8]. The low- and high-speed streaks span from the viscous sublayer, a thin region close to the wall where viscous dissipation dominates, to the adjacent so-called buffer layer. The quasi-streamwise vortices evolve in the buffer layer, around the streaks, and create upwash and downwash flows that (a) are biaxial extensional flows[5] and (b) contribute to the vertical transfer of momentum throughout the viscous, buffer and log layers.

The effect of polymers on turbulent wall-flow is to disrupt and modify the near-wall autonomous cycle of wall turbulence that results in a net drag reduction. Previous studies investigating polymer-vortex interactions [4–6] demonstrated that polymers primarily stretch (and extract energy) in the upwash and downwash regions generated by quasi-streamwise vortices and, consequently,
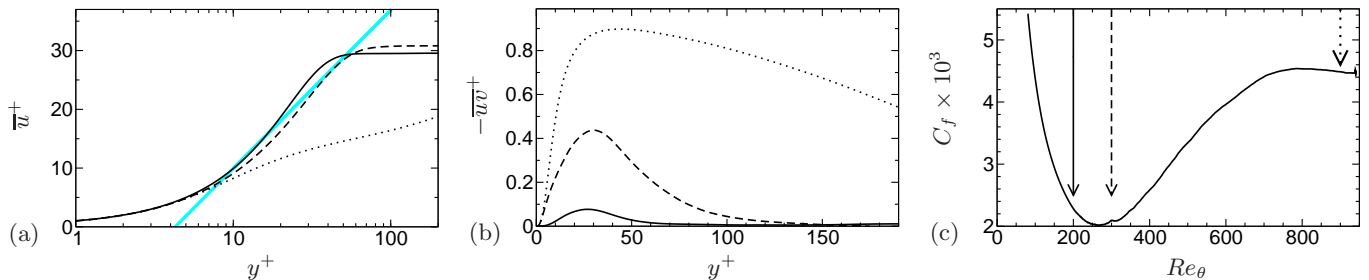
FIG. 1: Velocity statistics of the transitional boundary layer simulation of [7] for two states whose velocity profiles approach closely Virk's asymptotic velocity profile (Eq. 1). (a) Shows Eq. (1) ——— , $Re_\theta = 200$ ——— , $Re_\theta = 300$ - - - - , and $Re_\theta = 900$ ········ (fully turbulent flow). (b) Compares Reynolds shear stress, $-\overline{uv}^+$, for the three flow states as shown in (a). (c) Plots the distribution of the skin friction coefficient C_f as a function of the Reynolds number based on the local momentum thickness θ. Arrows point to the statistical profiles plotted in (a) and (b).

dampen the vortices. With increasing drag reduction, vortices become increasingly weaker and the high- and low-speed streaks become more coherent [9].

To best frame our hypothesis, let us first consider two thought experiments using polymers that possess the necessary elasticity to eradicate vortices. In the first experiment, consider that this polymer additive is suddenly added to fully-developed Newtonian turbulence (say by some injection scheme). Based on our understanding of polymer-turbulence interactions, it is expected that after an initial transient time in which coiled polymers become sufficiently stretched in the biaxial-extensional flows around vortices, the vortices will disappear but streaks will remain. Once all vortices are damped out, the stretching mechanism for polymers is limited to wall-shear and spanwise shear layers between streaks, both modest source of polymer stretching compared to biaxial-extensional flow [5]. Polymers therefore recoil, allowing instabilities to grow and new vortices to form. The emerging vortices grow until their biaxial-extensional flows become sufficiently strong to stretch the coiled polymers and the cycle repeats itself.

For the second thought experiment, let us consider a transitional flow of a polymer solution (i.e., a polymer ocean), again with the necessary elasticity to eradicate vortices. Since the turbulence-reducing mechanisms of polymers requires vortices to be effective, the impact of polymers on the linear region of the transition is expected to be marginal (note that polymers have no drag reducing effect on wall-bounded laminar flows). However, at the onset of the nonlinear breakdown of flow instabilities and the formation of vortices, the polymer drag reducing mechanisms are activated, the vortices become damped, and the flow is returned to a pre-breakdown transitional stage. This scenario is very much consistent with experimental results that show that polymer solutions that transition from laminar to MDR, stay at MDR as the Reynolds number is increased [10].

Based on the two thought experiments described

above, knowledge of the mechanisms of polymer-turbulence interactions, and the demonstrated existence of transitional states in a Newtonian fluid with velocity statistics similar to MDR, the hypothesis presented here is that a precise definition of MDR is that it is the transitional state that corresponds to the onset of the non-linear breakdown stage of transition. In practice, however, MDR turbulence corresponds to a narrow flow region centered about the onset of the nonlinear breakdown stage of transition that includes pre- and post-breakdown stages. We provide further substantiative evidence that this hypothesis is correct using direct numerical simulation of transition in a channel flow with polymer additives. The motivation to use a channel flow over a boundary layer simulation stems from the need to demonstrate a sustained MDR state. In a boundary layer, the required streamwise length scale of the domain for accurate computation and flow development is prohibitively large, whereas, a channel flow may be reasonably calculated over a very long time series.

Channel flow simulations are performed in a cartesian domain defined by the vector base $(\mathbf{e}_x, \mathbf{e}_y, \mathbf{e}_z)$ where x, y and z are the streamwise, wall-normal and spanwise directions, respectively. The components of the velocity vector $\mathbf{u}$ are u, v, and w. For a polymer solution, the flow transport equations are the conservation of mass, $\boldsymbol{\nabla} \cdot \mathbf{u} = 0$, and transport of momentum:

$$\frac{\partial \mathbf{u}}{\partial t} + (\mathbf{u} \cdot \boldsymbol{\nabla})\mathbf{u} = -\boldsymbol{\nabla} p + \frac{\beta}{Re}\nabla^2 \mathbf{u} + \frac{1-\beta}{Re}\boldsymbol{\nabla} \cdot \mathbf{T} + g(t)\mathbf{e}_x, \tag{2}$$

where $g(t) = -(dP/dx)$ is used to maintain constant mass flux. The parameter β is the ratio of solvent viscosity to the zero-shear viscosity of the polymer solution and affects both the viscous stress and polymer stress terms in Eq. (2). The polymer stress tensor $\mathbf{T}$ is computed using the FENE-P (Finite Elastic Non-linear Extensibility-Peterlin) model[11]:

$$\mathbf{T} = \frac{1}{We}\left(\frac{\mathbf{C}}{1 - \operatorname{tr}(\mathbf{C})/L^2} - \mathbf{I}\right), \tag{3}$$
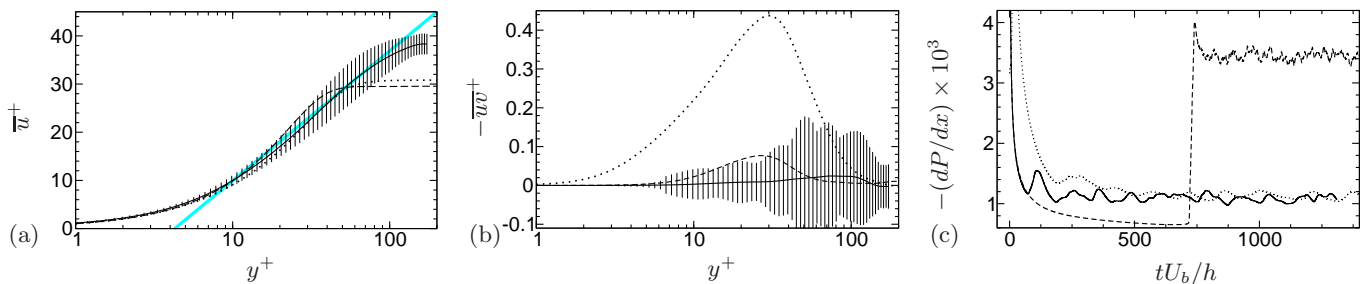
FIG. 2: Polymeric flows at MDR. (a) Shows MDR flow time and space-averaged mean velocity profile ——— and fluctuations of time-dependent, space-averaged mean velocity (error bars), Eq. (1) ——— , $Re_\theta = 200$ ---- , and $Re_\theta = 300$ ······· . (b) Compares Reynolds shear stress, for the three flow states as shown in (a). (c) Plots the time-evolution of pressure gradient for different flow and initial conditions: ---- Newtonian initiated with isotropic turbulent entrance flow (turbulent intensity $u'/U_b = 0.01$), ——— MDR flow ($L = 200, We_\tau = 720$) initiated with viscoelastic isotropic turbulent entrance flow ($u'/U_b = 0.005$), and ······· MDR flow ($L = 160, We_\tau = 200$) initiated from a fully developed turbulent channel flow with $\mathbf{C} = \mathbf{I}$ condition for the polymer field.

where the tensor $\mathbf{C}$ is the local conformation tensor of the polymer solution and $\mathbf{I}$ is the unit tensor. The properties of the polymer solution are β, the Weissenberg number based on the solution relaxation time λ and integral scales, $We = \lambda U_c / H$, or on viscous scales, $We_\tau = \lambda u_\tau^2 / \nu$, and the maximum polymer extension L. The FENE-P model assumes that polymers may be represented by a pair of beads connected by a non-linear spring and defined by the end-to-end vector $\mathbf{q}$. The conformation tensor is the phase-average of the tensorial product of the end-to-end vector $\mathbf{q}$ with itself, $\mathbf{C} = \langle \mathbf{q} \otimes \mathbf{q} \rangle$ whose transport equation is

$$\frac{\partial \mathbf{C}}{\partial t} + (\mathbf{u} \cdot \boldsymbol{\nabla})\mathbf{C} = \mathbf{C}(\boldsymbol{\nabla}\,\mathbf{u}) + (\boldsymbol{\nabla}\,\mathbf{u})^{\mathrm{T}}\mathbf{C} - \mathbf{T} \; . \quad (4)$$

On the left hand side of Eq. (4), the first two terms are responsible for the stretching of polymers by hydrodynamic forces, whereas the third term models the internal energy that tends to bring stretch polymers to their least energetic state (coiled). The FENE-P model has demonstrated its ability to capture the physics of polymer drag reduction [4, 12–15]. Eqs. (2-4) are solved using finite differences on a staggered grid and a semi-implicit time advancement scheme described elsewhere[16].

Here, we build on previous work[4, 16] in a channel flow at $Re_\tau = h u_\tau / \nu = 300$ simulated in a computational domain of dimensions $(20/3)h \times 2h \times (10/3)h$ or $2000 \times 600 \times 1000$ in Newtonian wall units, and with periodic conditions in x and z. The bulk Reynolds number $Re_b = U_b h / \nu$ is 5000 where U_b and h are the bulk velocity and channel half-height, respectively. Production runs were performed in a $256 \times 161 \times 256$ grid.

The initial flow and polymer conditions consist of a constant-mass flow, three-dimensional isotropic turbulence generated by Kolmogorov forcing[17]. The computational domain and grid are those of the channel with periodic conditions in the wall-normal direction. At time $t = 0$, the wall-normal boundary conditions are switched to no-slip to mimic the entrance of a channel flow, i.e. the

growth and merger of boundary layer, and a bypass transition induced by free stream turbulence similar to Wu & Moin[7]. The turbulent intensity of the initial condition is 0.5% for the polymer solution of interest.

A large parameter space was investigated with $L \in [100, 200]$ and $We_\tau \in [120, 720]$. All simulations for $We_\tau \geq 120$ and $L \geq 160$ or $We_\tau \geq 300$ and $L \geq 100$ lead to drag reduction in the range 68 to 72% and mean velocity profiles in close agreement with Virk's asymptotic profile. This extensive study will be discussed in future publications. This letter focuses on one simulation with $L = 200$ and $We_\tau = 720$, whose Reynolds shear stress is similar to simulations for $We_\tau \geq 200$.

The mean velocity and Reynolds shear stress of our polymeric simulation were averaged over homogenous directions and a time duration of $1500h/U_b$ of the MDR flow at steady-state. In order to evaluate the envelope of MDR turbulence (i.e., the extent over which the flow oscillates around MDR), we compute both time- and space-averaged quantities (denoted by $\overline{\bullet}$) and time-dependent quantities averaged over homogenous directions (denoted by $\langle \bullet \rangle_{(t)}$). The latter statistics are calculated over 300 successive snapshots, separated by $5h/U_b$. The largest positive and negative deviations of $\langle u \rangle_{(t)}$ and $- \langle uv \rangle_{(t)}$ from $\overline{u}$ and $-\overline{uv}$ are displayed in Fig. 2 by error bars. Fig. 2a compares our simulation's mean velocity profile to Eq. (1) and the Newtonian transition data of Fig. 1. The agreement with Virk is excellent and the error bars span across Wu & Moin's $Re_\theta = 200$ to 300 states. The Reynolds shear stress $-\overline{uv}$ in Fig. 2b is essentially negligible, yet the largest deviations of $- \langle uv \rangle_{(t)}$ exhibit magnitude slightly larger than the $Re_\theta = 200$ Newtonian transitional state. The largest negative and positive deviations of the mean velocity profiles are, not surprisingly, found to correlate with lower and higher values of $-dP/dx$ or drag, whose time evolution is shown in Fig. 2c. Conversely, the largest positive deviations of $- \langle uv \rangle_{(t)}$ are correlated to higher drag event. Fig. 2c
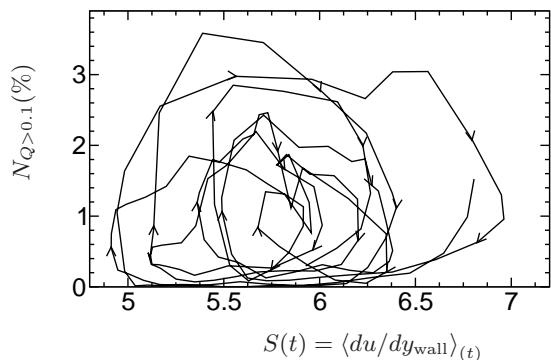
FIG. 3: Orbits of spatially-averaged wall shear in the lower wall of the channel as a function of the volume fraction of the flow region in lower half of the channel occupied by vortices identified by positive regions of the second invariant, $Q > 0.1$, of the velocity gradient[19].

shows that, for both initial conditions envisioned in our two thought experiments (fully developed turbulent flow and entrance flow), the flow oscillates between these lower and higher drag events around MDR, as anticipated by our thought experiments. Interestingly, the polymeric transition breaks down earlier than Newtonian flows with higher initial turbulent intensities, which is indicative of a possible destabilizing polymeric effects on (pre-breakdown) streaks[4, 18].

Another illustration of the oscillatory nature of MDR turbulence is provided in Fig. 3, which plots the volume fraction N_Q occupied by vortices (identified using the Q criterion[19]) in the lower half of the channel as a function of the spatially averaged wall shear $S(t) = \langle du/dy_{\mathrm{wall}} \rangle_{(t)}$. Owing to the inherent subjectivity of threshold selection in any other vortex identification technique[19], we tested

several threshold in the range $Q \in [0.01, 1]$ and verified that (a) all thresholds gave orbits consistent with Fig. 3 and (b) the chosen threshold $Q = 0.1$ depicts regions where velocity vectors exhibit a rotational pattern. The temporal evolution of $N_{Q>0.1} = f(S(t))$ shows clockwise-rotating orbits centered roughly around the time-averaged wall shear $\overline{S} = 5.7$. For a typical orbit, starting from a vortex-free state, (i.e., $N_Q = 0$), the wall shear decreases to a local minimum, lower that the mean wall shear, at which point vortices appear and grow (i.e., $N_Q > 0$). As vortices grow, the wall shear increases. Eventually, vortices are dampened, shown by the reduction of N_Q. The wall shear continues to increase toward a local maximum until $N_Q \sim 1\%$, and then decreases back to a local minimum as the vortical activity disappears.

In conclusion, this letter uniquely defines polymer maximum drag reduction as the transitional state that corresponds to the onset of the nonlinear breakdown stage of transition. Furthermore, MDR turbulence corresponds to oscillations between pre- and post-breakdown stages. These results not only provide a precise definition of MDR they also explain observed differences between experimental data sets at MDR. This letter also achieves a critical step in the progress toward developing predictive models of polymer drag reduction, as it narrows the research focus on intermittence and transitional flows.

[1] P. Virk, H. Mickley, and K. Smith, Trans. ASME E: J. Appl. Mech. **37**, 488 (1970).
[2] M. Warholic, G. Schmidt, and T. Hanratty, J. Fluid Mech. **388**, 1 (1999).
[3] P. K. Ptasinski, F. T. M. Nieuwstadt, B. H. A. A. Van den Brule, and M. A. Hulsen, Flow, Turbulence and Combustion **66**, 159 (2001).
[4] Y. Dubief, C. White, V. Terrapon, E. Shaqfeh, P. Moin, and S. Lele, J. Fluid Mech. **514**, 271 (2004).
[5] V. Terrapon, Y. Dubief, P. Moin, E. Shaqfeh, and S. Lele, J. Fluid Mech. **504**, 61 (2004).
[6] K. Kim, C. Li, R. Sureshkumar, S. Balachandar, and R. Adrian, J. Fluid Mech. **584**, 281 (2007).
[7] X. Wu and P. Moin, J. Fluid Mech. **630**, 5 (2009).
[8] J. Jiménez and A. Pinelli, J. Fluid Mech. **389**, 335 (1999).
[9] C. White, V. Somandepalli, and M. Mungal, Exp. Fluids **36**, 62 (2004).
[10] P. Virk, AIChE Journal **21**, 625 (1975).
[11] R. Bird, R. Armstrong, and O. Hassager, *Dynamics of Polymeric Liquids. Vol. 2: Kinetic Theory* (Wiley-Interscience, 1987,, 1987).
[12] R. Sureshkumar, A. Beris, and R. Handler, Phys. Fluids **9**, 743 (1997).
[13] E. De Angelis, C. Casciola, and R. Piva, Computers & Fluids **31**, 495 (2002).
[14] P. Ptasinski, B. Boersma, F. Nieuwstadt, M. Hulsen, B. Van Den Brule, and J. Hunt, J. Fluid Mech. **490**, 251 (2003).
[15] T. Min, H. Choi, and J. Yoo, J. Fluid Mech. **492**, 91 (2003).
[16] Y. Dubief, V. Terrapon, C. White, E. Shaqfeh, P. Moin, and S. Lele, Flow, turbulence and combustion **74**, 311 (2005).
[17] G. Boffetta, A. Celani, and A. Mazzino, Phys. Rev. E **71**, 036307 (2005).
[18] Y. Dubief, C. M. White, E. S. G. Shaqfeh, and V. E. Terrapon, in *Annual Research Briefs* (Center for Turbulence Research, Stanford, CA, 2010), pp. 395–404.
[19] Y. Dubief and F. Delcayre, J. of Turbulence **1** (2000).